

## Review article

## Right ventricular dysfunction: pathophysiology, experimental models, evaluation, and treatment

Carlos Real,<sup>a,b,◇</sup> Carlos Nicolás Pérez-García,<sup>a,◇</sup> Carlos Galán-Arriola,<sup>a</sup> Inés García-Lunar,<sup>a,c,d</sup> and Ana García-Álvarez<sup>a,d,e,f,\*</sup><sup>a</sup> Centro Nacional de Investigaciones Cardiovasculares Carlos III (CNIC), Madrid, Spain<sup>b</sup> Servicio de Cardiología, Hospital Universitario Clínico San Carlos, Madrid, Spain<sup>c</sup> Servicio de Cardiología, Hospital Universitario La Moraleja, Madrid, Spain<sup>d</sup> Centro de Investigación Biomédica en Red de Enfermedades Cardiovasculares (CIBERCV), Spain<sup>e</sup> Servicio de Cardiología, Instituto Clínic Cardiovascular (ICCV), Hospital Clínic, Barcelona, Spain<sup>f</sup> Universitat de Barcelona, Barcelona, Spain

## Article history:

Received 25 February 2024

Accepted 28 May 2024

Available online 26 July 2024

## Keywords:

Right ventricle

Right ventricular dysfunction

Experimental models

## Palabras clave:

Ventrículo derecho

Disfunción ventricular derecha

Modelos experimentales

## ABSTRACT

Interest in the right ventricle has substantially increased due to advances in knowledge of its pathophysiology and prognostic implications across a wide spectrum of diseases. However, we are still far from understanding the multiple mechanisms that influence right ventricular dysfunction, its evaluation continues to be challenging, and there is a shortage of specific treatments in most scenarios. This review article aims to update knowledge about the physiology of the right ventricle, its transition to dysfunction, diagnostic tools, and available treatments from a translational perspective.

© 2024 Sociedad Española de Cardiología. Published by Elsevier España, S.L.U. This is an open access article under the CC BY-NC-ND license (<http://creativecommons.org/licenses/by-nc-nd/4.0/>).

## Disfunción del ventrículo derecho: fisiopatología, modelos experimentales, evaluación y tratamiento

## RESUMEN

El interés por el ventrículo derecho ha aumentado significativamente gracias a los avances en el conocimiento de su fisiopatología e impacto pronóstico en un gran espectro de enfermedades. Sin embargo, todavía nos encontramos lejos de entender los múltiples mecanismos que influyen en su disfunción; su evaluación sigue planteando retos, y continuamos sin disponer de tratamientos específicos en la mayoría de los escenarios. Esta revisión pretende, desde una perspectiva traslacional, actualizar los conocimientos sobre la fisiología del ventrículo derecho, y su transición a la disfunción, las herramientas diagnósticas y los tratamientos disponibles.

© 2024 Sociedad Española de Cardiología. Publicado por Elsevier España, S.L.U. Este es un artículo Open Access bajo la licencia CC BY-NC-ND (<http://creativecommons.org/licenses/by-nc-nd/4.0/>).

## Abbreviations

LV: left ventricular

PA: pulmonary artery

PH: pulmonary hypertension

RA: right atrial

RV: right ventricular

## INTRODUCTION

In recent decades, there has been growing recognition of the crucial role played by right ventricular (RV) dysfunction in the functional status and outcomes of multiple diseases with incidences of RV dysfunction exceeding 50%.<sup>1</sup> These diseases include left heart failure (HF),<sup>2</sup> pulmonary arterial hypertension (PAH),<sup>3</sup> congenital heart diseases, and cardiomyopathies.<sup>4–6</sup> The damage to the RV in these different settings, as well as the underlying pathophysiological mechanisms and molecular pathways, has been illuminated via experimental models. At the same time, cardiac imaging has evolved to enable an accurate assessment of the anatomy and function in these varied conditions and even permits their early diagnosis through myocardial deformation and tissue characterization techniques. This progress has led to improved research into new therapeutic targets, the spread of percutaneous techniques, and the refinement of interventional

\* Corresponding author.

E-mail addresses: [anagarci@clinic.cat](mailto:anagarci@clinic.cat), [ana.garcia@cnic.es](mailto:ana.garcia@cnic.es) (A. García-Álvarez).✉ [@carlosreal42](mailto:@carlosreal42), [@AnaGarcAlvarez2](mailto:@AnaGarcAlvarez2), [@CarlosNicolsPr3](mailto:@CarlosNicolsPr3), [@cgalanarriola](mailto:@cgalanarriola),

@CNIC\_CARDIO

◇ Both authors contributed equally to this work.

indications aimed at preventing the irreversible damage associated with such diseases. However, we are far from understanding the multiple mechanisms influencing RV dysfunction, its evaluation still poses challenges, and specific treatments are still lacking for most patients, indicating the need for further research. The present review aims to use a translational perspective to update knowledge about RV physiology under normal conditions and its transition to dysfunction in different settings, as well as the diagnostic tools and available treatments.

## RIGHT VENTRICULAR EMBRYOLOGY, ANATOMY, AND PHYSIOLOGY

The right ventricle differs from the left ventricle in many ways, including its embryonic origin. This difference helps to explain the associated congenital heart diseases and possibly why different signaling pathways are activated in the 2 chambers in response to the same insult. The right ventricle originates from the secondary (or anterior) heart field, while the left ventricle arises from the primary heart field. The cells of the primary field form the primitive heart tube, which expands anteriorly from cells derived from the secondary field (figure 1A). In the embryo and fetus, the right ventricle is the dominant chamber responsible for ~60% of the cardiac output, delivering systemic perfusion via the foramen ovale and ductus arteriosus. At birth, with the closure of both of these channels, the outputs of both ventricles equalize, and the right ventricle adapts to pumping blood solely to the pulmonary circulation (under low pressure), which is why the RV wall narrows during the first year of life.

Anatomically, the right ventricle is anterior and immediately behind the sternum; its wall is thin (2–3 mm) and its chamber has a half-moon shape, accommodating a volume 10% to 15% greater than that of the left ventricle. The right ventricle can be subdivided

into 3 parts (figure 1B): an inflow tract, which includes the tricuspid valve, chordae tendineae, and papillary muscles (3 or more); a trabeculated apical myocardium; and an infundibulum or outflow tract, a tubular muscular structure that supports the pulmonary valve. The supraventricular crest separates the inflow and outflow tracts and extends along the interventricular septum toward the insertions of the anterior papillary muscles, forming the moderator band. The RV wall is composed of 2 layers of muscle cells (figure 1C): the internal or subendocardial layer, which exhibits a longitudinal orientation extending from the apex to the papillary muscles and outflow tract; and the external or superficial layer, which is characterized by a circumferential orientation that continues through the septum with the superficial layer of the left ventricle. This continuity of fibers, the shared interatrial septum, and the surrounding pericardium contribute to ventricular interdependence.

The normal function of the right ventricle depends on systemic venous return, afterload, diastolic function, RV free wall and interventricular septum contractility, and pericardial distensibility. Afterload refers to the wall stress during systolic ejection and is the sum of the resistive component and pulsatile blood flow. Indeed, the right ventricle and the pulmonary circulation should be considered a combined functional unit. RV contractility results from the contraction of the longitudinal fibers, which brings the tricuspid valve and apex closer together; the contraction of the circumferential fibers, which moves the free wall toward the septum; and the traction exerted by the RV insertion points on the left ventricle, which are triggered by left ventricular (LV) contraction. Under physiological conditions, contraction is predominantly longitudinal; however, under significant afterload or after cardiac surgery,<sup>7</sup> longitudinal displacement decreases and transverse contraction increases. The right ventricle is largely perfused by the right coronary artery through its marginal (free wall) and conal (infundibulum) branches. Compared with the left

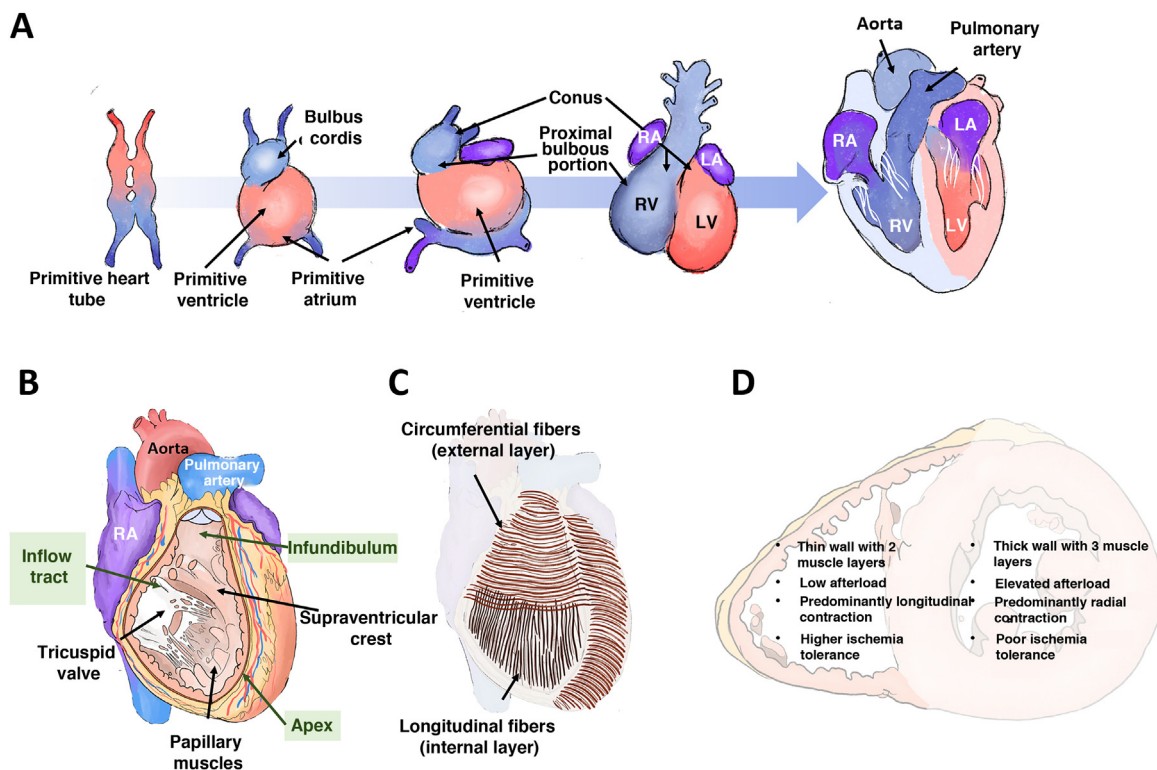


**Figure 1.** Right ventricular embryology, anatomy, and physiology. A: origin and embryonic development of both ventricles. B: right ventricular anatomy. C: arrangement of the muscle fibers. D: main differential characteristics between the 2 ventricles. LA, left atrium; LV, left ventricle; RA, right atrium; RV, right ventricle.

ventricle, the right ventricle is more resistant to ischemia due to a more balanced coronary flow during systole and diastole, lower oxygen extraction, a more extensive network of collaterals,<sup>8</sup> and higher myocardial expression of aerobic glycolytic enzymes.<sup>9</sup> The main characteristic differences between the 2 ventricles are summarized in figure 1D.

## PATHOPHYSIOLOGY OF RIGHT VENTRICULAR DYSFUNCTION

Three basic pathophysiological mechanisms can be distinguished (table 1 and figure 2): pressure overload, volume overload, and myocardial disease. All 3 frequently coexist. Other mechanisms include diastolic dysfunction and ventricular interdependence. A recent study<sup>10</sup> involving the hemodynamic assessment of RV filling in patients with pulmonary hypertension (PH) and experiments in isolated cardiomyocytes revealed the role of diastolic dysfunction and the novel concept of right atrial (RA)-RV uncoupling, calculated as RA minimal volume/RV end-diastolic volume. Ventricular interdependence, known from classic studies in experimental animal models,<sup>11</sup> refers to the ability of the size, contractility, and distensibility of one ventricle to affect the other ventricle via direct mechanical interactions. About 20% to 40% of the RV systolic volume is due to the contraction of the left ventricle. Conversely, displacement of the septum toward the left ventricle and the fall in the systolic volume of the right ventricle reduces the LV preload, which contributes to peripheral hypoperfusion. Finally, the diastolic ventricular interaction is understood as the competition between the distensibility and filling of both ventricles within the confined pericardial space.

### Right ventricle with pressure overload

The right ventricle is not designed to tolerate acute afterload increases, and its impact on the reduction in systolic volume is much greater than that of the left ventricle.<sup>11</sup> Accordingly, under sudden elevations in afterload conditions, such as during pulmonary embolism, cardiac output can initially be maintained via a compensatory increase in heart rate and contractility. However, persistence of the condition leads to ventricular dilatation, tricuspid regurgitation due to annular dilatation, and systolic

dysfunction, with characteristic hypokinesia and akinesia of the basal and medial free wall and relative apical hypercontractility (McConnell's sign). In severe cases, as a consequence of ventricular interdependence, the LV preload is reduced, triggering circulatory collapse. Under chronic pressure overload conditions, the right ventricle initially adapts via progressive concentric hypertrophy, which permits preservation of contractile volumes and function (homeometric adaptation). However, over time, this mechanism becomes exhausted and the right ventricle undergoes maladaptive remodeling characterized by eccentric hypertrophy, dilatation, end-systolic interventricular septal flattening, and intra- and interventricular dyssynchrony (heterometric adaptation). Taken together, this leads to progressive uncoupling from the pulmonary artery (PA) and subsequent right HF.<sup>12</sup> The initial adaptive response is possible due to the ability of cardiomyocytes to detect and respond to conformational changes by increasing load (mechanotransduction)<sup>13</sup> and to neurohormonal and paracrine signals from adjacent fibroblasts by inducing the expression of fetal genes, such as myosin heavy chain  $\beta$ , characterized by lower energy requirements but lower contractile capacity than the  $\alpha$  form.<sup>14</sup> In this RV adaptation, the pulsatile or impedance component of the PA plays a vital role and is independent of the resistive component (pulmonary vascular resistance [PVR]).<sup>15</sup> This fact, sometimes overlooked in the clinic, was identified in classic preclinical studies that revealed how the stiffness of the PA (and, thus, the pulsatile component of afterload) was a greater determinant of RV hypertrophy than PA pressure (PAP).<sup>16</sup>

At the histological level, hypertrophy and disorganization of the cardiomyocytes occur, as well as hypertrophy of the coronary artery media, lymphocyte infiltration, and connective tissue deposition. In advanced stages, ischemia develops due to the imbalance between the increased oxygen demand and the altered coronary artery perfusion resulting from higher wall tension, limited diastole due to increased RV pressure, vascular remodeling, and concomitant capillary rarefaction. The neurohormonal activation, inflammation, and ischemia culminate in greater myocardial fibrosis, which contributes to RV-PA uncoupling.<sup>17</sup> Nonetheless, the extent of fibrosis in the right ventricle is lower than that in the left ventricle subjected to pressure overload and is more focal, with a predominance at the insertion points, where the mechanical stress is greater.<sup>18</sup> This phenomenon explains the frequent

**Table 1**  
Causes of right ventricular dysfunction by pathophysiological mechanism

	Pressure overload	Volume overload	Myocardial disease
Acute causes	<ul style="list-style-type: none"> <li>- Acute pulmonary embolism</li> <li>- Acute left HF</li> <li>- Mechanical ventilation with positive pressure</li> <li>- Acute hypoxia (eg, acute respiratory distress syndrome in adults)</li> <li>- Acidosis</li> </ul>	<ul style="list-style-type: none"> <li>- Acute TR and PR (eg, infectious endocarditis, trauma)</li> <li>- High acute cardiac output (eg, thyrotoxicosis)</li> <li>- Excessive fluid replacement or massive transfusion</li> </ul>	<ul style="list-style-type: none"> <li>- AMI with RV involvement</li> <li>- Acute myocarditis</li> <li>- Postpericardiotomy syndrome</li> <li>- After left ventricular assist device implantation</li> <li>- Cardiotoxicity</li> <li>- Sepsis</li> </ul>
Chronic causes	<ul style="list-style-type: none"> <li>- Stenosis of the RV outflow tract (eg, unrepaired tetralogy of Fallot)</li> <li>- Systemic right ventricle with transposition of the great arteries repaired using atrial switch operation or in congenitally corrected forms that have not undergone surgical repair</li> <li>- Pulmonary stenosis (valvular, infundibular, supra- or peripheral arterial branches)</li> <li>- Constrictive pericarditis</li> <li>- Chronic PH</li> </ul>	<ul style="list-style-type: none"> <li>- Chronic TR</li> <li>- Chronic PR (eg, repaired tetralogy of Fallot with residual PR)</li> <li>- Left-right intracardiac shunts (eg, atrial septal defect)</li> <li>- Arteriovenous fistulas</li> <li>- Anomalous pulmonary venous drainage</li> </ul>	<ul style="list-style-type: none"> <li>- Chronic ischemic heart disease</li> <li>- Cardiotoxicity</li> <li>- Cardiomyopathies:               <ul style="list-style-type: none"> <li>• Dilated</li> <li>• Hypertrophic</li> <li>• Restrictive</li> <li>• Arrhythmogenic RV cardiomyopathy</li> <li>• Amyloidosis</li> <li>• Inflammatory/granulomatosis (sarcoidosis)</li> <li>• Due to other deposits (eg, Danon, Fabry, Pompe)</li> <li>• Ebstein anomaly</li> </ul> </li> </ul>

AMI, acute myocardial infarction; HF, heart failure; PH, pulmonary hypertension; PR, pulmonary regurgitation; RV, right ventricular; TR, tricuspid regurgitation.

**Pathophysiology, diagnosis, and management of right ventricular dysfunction**

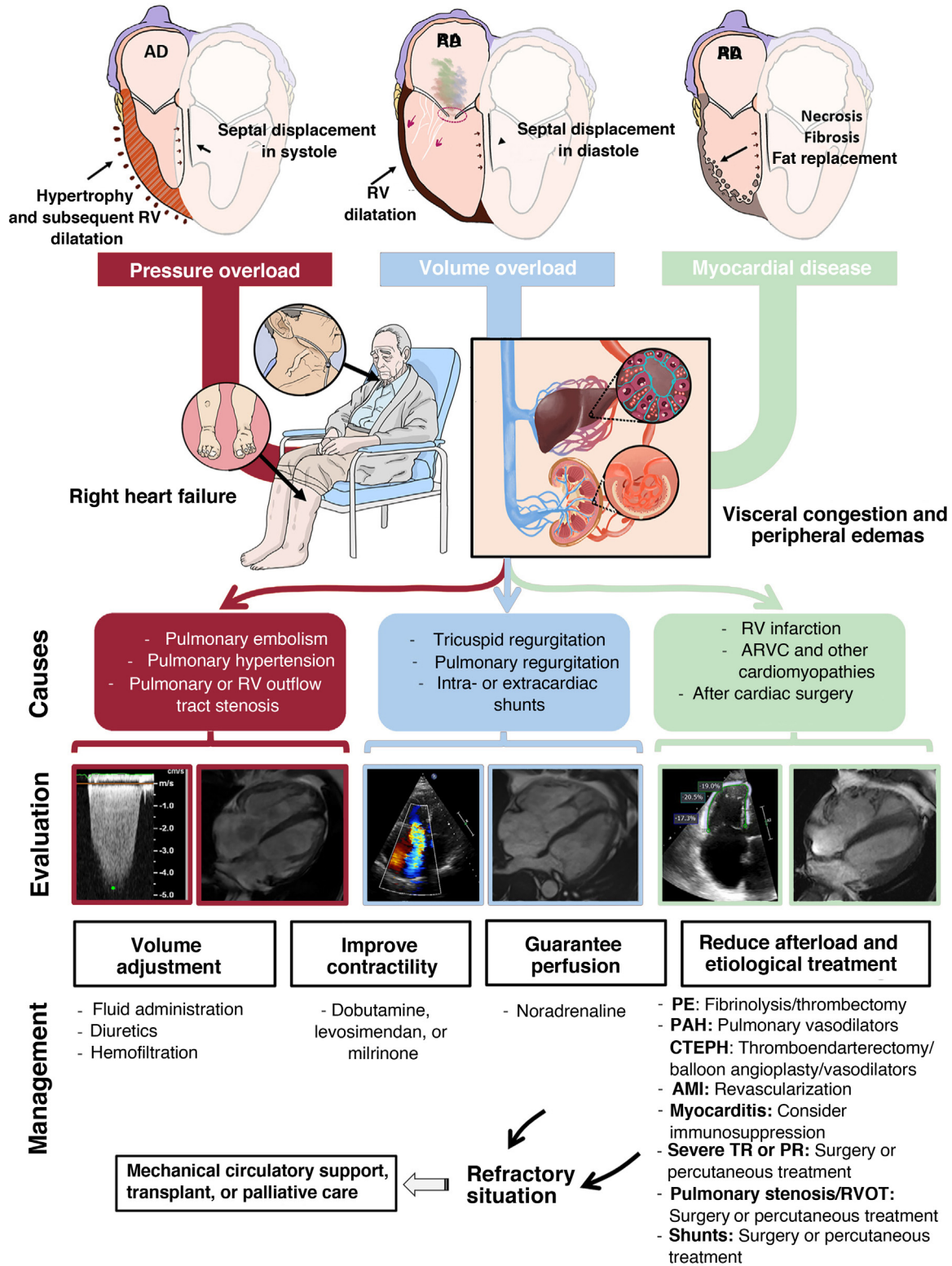


**Figure 2.** Central illustration. Pathophysiology, diagnosis, and management of right ventricular dysfunction. AMI, acute myocardial infarction; ARVC, arrhythmogenic right ventricular cardiomyopathy; CTEPH, chronic thromboembolic pulmonary hypertension; PAH, pulmonary arterial hypertension; PE, pulmonary embolism; PR, pulmonary regurgitation; RA, right atrium; RV, right ventricular; RVOT, right ventricular outflow tract; TR, tricuspid regurgitation. Cardiac magnetic resonance imaging of volume overload courtesy of Dr Amparo Esteban, Hospital Universitario La Moraleja.

functional recovery of the right ventricle after a thromboendarterectomy or lung transplant.<sup>19</sup> During this entire process, experimental<sup>20</sup> and clinical<sup>21</sup> evidence has shown pertinent metabolic changes, particularly the replacement of fatty acid oxidation by anaerobic glycolysis as a source of adenosine triphosphate, which may lead to the adaptive response of the right ventricle independently of the severity of the pressure overload.

### Right ventricle with volume overload

At the structural level, persistent volume overload leads to progressive RA and RV dilatation. This results in septal flattening and displacement to the left during diastole and increased myocardial mass with preserved wall thickness. Contractility can be maintained for extended periods (heterometric adaptation)<sup>22</sup> but eventually deteriorates in advanced stages, often irreversibly. This deterioration leads to peripheral and visceral venous congestion, particularly affecting the hepatic and renal systems. These changes are key to the pathogenesis of cardiorenal and cardiohepatic syndromes, which are the final manifestations of all severe RV dysfunction from any cause.

At the molecular level, volume overload shares pathways with pressure overload, such as the reactivation of fetal genes, activation of proinflammatory and profibrotic pathways, and a metabolic shift to glycolysis.<sup>23</sup> In recent years, this condition has gained relevance due to the increase in percutaneous interventions aimed at treating severe tricuspid regurgitation, with indications for these interventions and devices depending on the degree of RV dysfunction (table 2).<sup>24–30</sup> Another major cause of RV volume overload is pulmonary regurgitation after tetralogy of Fallot repair, which is the primary indication for reintervention during follow-up.<sup>26</sup> Surgery is associated with low postoperative mortality and

favorable long-term outcomes, as long as it is performed before the RV dysfunction becomes irreversible and before there is a high risk of ventricular arrhythmias and sudden cardiac death.<sup>31</sup>

Finally, septal defects are a relatively frequent cause of volume overload. The decision to proceed with surgical or percutaneous device closure is equally determined by biventricular function and PVR (table 2).

### Right ventricle with myocardial disease

Myocardial disease refers to intrinsic myopathy of the right ventricle that alters its contractility or relaxation. The most prominent acute causes (table 1) include myocardial infarction, myocarditis, and postpericardiotomy syndrome. In the chronic setting, the classic paradigm is arrhythmogenic RV cardiomyopathy, characterized by fibrofatty replacement, initially affecting the basal segments of the right ventricle and, in more advanced forms, the apical segments.<sup>32</sup> The predominant cause is mutations in genes encoding desmosomal proteins that control cardiomyocyte adhesion, with plakophilin-2 being the most frequently affected. However, the molecular mechanisms underlying the cardiomyocyte loss, fibrosis, adipogenesis, inflammation, and arrhythmic risk remain unclear.

In this regard, the development of experimental models has helped to identify signaling pathways, such as the WNT pathway, the Hippo-Yes-associated protein pathway, peroxisome proliferator-activated receptor  $\gamma$ , and microRNAs.<sup>33</sup> RV involvement is also frequent in other cardiomyopathies and is associated with a worse prognosis.<sup>5,34</sup> Prevalence rates are 30% in dilated cardiomyopathy,<sup>6</sup> 5% in hypertrophic cardiomyopathy,<sup>35</sup> 60% in cardiac amyloidosis,<sup>34</sup> and 15% to 20% in sarcoidosis.<sup>36</sup>

**Table 2**

Morphofunctional parameters of the right ventricle with impact on treatment decisions and risk stratification

Clinical setting	Morphofunctional RV parameters	Strategy to follow
Acute pulmonary embolism <sup>24</sup>	TAPSE < 16 mm, tricuspid S' < 9.5 cm/s, or RV/LV ratio $\geq$ 1 on TTE or CT	Classifies patients as having moderate-to-high risk and consequently requiring hospitalization, monitoring, and assessment of fibrinolysis or transcatheter treatments based on the hemodynamic situation and course
Severe tricuspid regurgitation	RVEF > 45% (associated with RV symptoms or dilatation)	Consider surgical or percutaneous tricuspid repair or replacement (edge-to-edge) <sup>25</sup>
	RV dilatation or symptoms with RVEF 30%-45%	Consider bicaval valve implantation or medical therapy <sup>25</sup>
	RVEF < 30% or end-stage right HF	Contraindicated: surgical or percutaneous tricuspid repair or replacement
Severe pulmonary regurgitation (repaired tetralogy of Fallot) <sup>26</sup>	RV end-systolic volume index $\geq$ 82 mL/m <sup>2</sup> , RV/LV end-diastolic volume ratio > 2, or RVEF < 47% on CMR <sup>27</sup>	Indication for surgical or transcatheter pulmonary valve replacement in patients without native RV outflow tract and amenable anatomy
Ebstein anomaly <sup>26</sup>	If progressive dilatation or deterioration of RV systolic function	Consider surgical repair, even in asymptomatic patients
	If severe RV dysfunction, preserved LV ejection fraction, and normal left pressure	Bilateral cavopulmonary anastomosis (Glenn)
Interatrial communication <sup>26</sup>	RV volume overload Qp/Qs > 1.5, PVR < 3 WU, and normal left function	Surgical or percutaneous closure is indicated
Arrhythmogenic cardiomyopathy	RVEF < 40%	High-risk criteria for SCD. Consider ICD (class IIa)
Durable ventricular assist device implantation	- PAPi (sPAP – dPAP/central venous pressure) < 2 - RAP/pulmonary capillary pressure > 0.63 - RV stroke work index (0.0136 $\times$ stroke volume index $\times$ [mPAP – RAP]) < 8-12 h/m/beat/m <sup>2</sup> - EUROMACS <sup>28</sup> > 4 - U-Penn <sup>29</sup> = 6-6.7 (moderate risk) and > 6.7 (high risk)	All of these conditions lead to acute risk of acute postimplant RV dysfunction. If $\geq$ 2 coexist, there is an elevated risk of complications <sup>30</sup>

CMR, cardiac magnetic resonance; CT, computed tomography; dPAP, diastolic pulmonary arterial pressure; ICD, implantable cardioverter-defibrillator; LV, left ventricular; mPAP, mean pulmonary arterial pressure; PAPi, pulmonary artery pulsatility index; PVR, pulmonary vascular resistance; RAP, right atrial pressure; RV, right ventricular; RVEF, right ventricular ejection fraction; SCD, sudden cardiac death; sPAP, systolic pulmonary arterial pressure; TAPSE, tricuspid annular plane systolic excursion; TTE, transthoracic echocardiography; WU, Wood units.

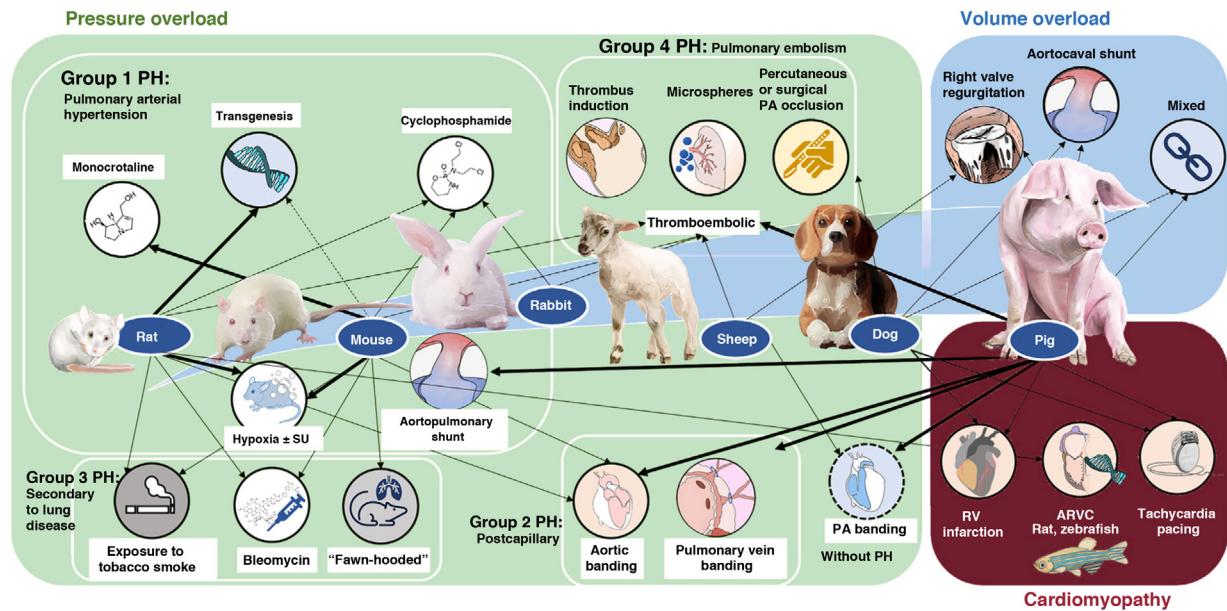


**Figure 3.** Experimental animal models of right ventricular dysfunction. ARVC, arrhythmogenic right ventricular cardiomyopathy; PA, pulmonary artery; PH, pulmonary hypertension; RV, right ventricle; SU, Sugen. Arrow thickness reflects the popularity of these models.

Finally, notable cardiomyopathic mechanisms include Ebstein anomaly, in which apical displacement of the tricuspid valve and atrialization of the right ventricle result in a functionally hypoplastic right ventricle that becomes dysfunctional. This condition is exacerbated by the presence of tricuspid regurgitation and other frequently associated abnormalities (septal defects and pulmonary atresia or stenosis).

## EXPERIMENTAL MODELS OF RIGHT VENTRICULAR DYSFUNCTION

Experimental animal models allow the molecular study of pathophysiological mechanisms and, in the case of large animals, their characterization via diagnostic and therapeutic techniques similar to those used in clinical practice.<sup>37</sup> The most frequently used species are rodents (mainly mice and rats) due to their low cost, high fertility, and, in the case of mice, their amenability to genetic manipulation. Large animal models, particularly pigs, have a more translational focus<sup>38–41</sup> but are more expensive to maintain.

Figure 3 shows the main animal models classified by the type of RV pressure overload (associated with PH or not), volume overload, and myocardial disease. Their advantages and disadvantages are detailed in table 3. In the case of pressure overload, the most commonly used rodent models are hypoxia alone or combined with the vascular endothelial growth factor receptor antagonist Sugen, the monocrotaline pyrrole model of lung toxicity, and transgenic models. In our experience, porcine pressure overload models are highly useful for validating diagnostic models and evaluating treatments, given the anatomical and physiological similarities between pigs and humans.

Figure 4<sup>18,20,38–45</sup> shows the schemes, advanced imaging characterization, and main contributions of these models, which can be created using an aortopulmonary shunt,<sup>40</sup> banding of the pulmonary veins,<sup>18,38,39,41–44</sup> stenosis of the PA,<sup>20</sup> and microsphere embolization.<sup>44,45</sup> These and other models have helped to identify distinct molecular pathways related to RV dysfunction in PH, which include tissue damage (oxidative stress, fibrosis, and

apoptosis), activation of maladaptive processes (inflammation and fibrosis), and, at the cellular level, hypertrophy, metabolic switch, and mitochondrial dysfunction.<sup>46</sup> In addition, animal models have recently proved useful for assessing therapeutic targets in diseases such as PAH<sup>32,39,41</sup> and arrhythmogenic RV cardiomyopathy.<sup>33</sup>

## ASSESSMENT OF RIGHT VENTRICULAR DYSFUNCTION

RV dysfunction typically presents with nonspecific symptoms such as fatigue, abdominal distension, and anorexia.<sup>3</sup> In the physical examination, jugular venous distension can be detected, as well as pleural effusion, ascites, lower limb edema, hepatomegaly, and hepatojugular reflux (figure 2). Natriuretic peptides and troponin can be useful for identifying and monitoring RV dysfunction, although they are also elevated (and to a greater extent) in LV dysfunction and it is impossible to differentiate the level of injury between the 2 ventricles.<sup>47</sup> Alterations in hepatic and renal blood profiles are pertinent in patients with congestion or low output. Chest radiography can reveal cardiomegaly due to enlargement of the right heart border. Electrocardiography frequently shows deviation of the axis to the right ( $> 90^\circ$ ), P pulmonale waves, prominent R waves in V<sub>1</sub> and S waves in V<sub>5</sub> and V<sub>6</sub>, as well as the presence of atrial fibrillation. Acute pulmonary embolism is usually associated with sinus tachycardia, T wave inversion in V<sub>1</sub> to V<sub>3</sub>, the S1Q3T3 pattern, or right bundle branch block.

Cardiopulmonary exercise testing is a useful tool for assessing the functional capacity of patients with right HF. Its use has become more widespread in the prognostic stratification of PAH (where a peak  $\text{VO}_2 < 11 \text{ mL/min/kg}$  [ $< 35\%$  of predicted] and a  $\text{VE}/\text{VCO}_2$  at anaerobic threshold  $> 44$  are associated with annual mortality  $> 20\%$ ).<sup>3</sup> It is also used in deciding on the repair of pulmonary regurgitation after tetralogy of Fallot repair,<sup>31</sup> and in arrhythmogenic RV cardiomyopathy, in which a  $\text{VE}/\text{VO}_2 > 34$  has been associated with higher risk of HF and worse heart transplant-free survival.<sup>48</sup>

**Table 3**  
Experimental models of right ventricular dysfunction

	Model	Animal	Advantages	Disadvantages
<i>Pressure overload</i>				
Pressure overload with PH	Monocrotaline	Rat	Simplicity, low cost	Myocardial and systemic toxicity; little translational value
	Hypoxia	Mouse, rat	Simplicity, low cost	Mild hemodynamic effect; reversible with normoxia
	Hypoxia + Sugen	Rat	Simplicity, low cost, greater RV hemodynamic severity and effect than hypoxia alone	Myocardial toxicity of Sugen and interference of the endothelial growth factor pathway with pathophysiology
	Fawn-hooded (spontaneous PH associated with chromosomal abnormality)	Rat	Similar characteristics to human PAH	Limited availability; little translational value
	Transgenic ( <i>BMPR-2</i> KO, deficiency in <i>LRP1</i> , <i>PPAR<math>\gamma</math></i> , <i>TGF<math>\beta</math>1</i> )	Mouse	Useful for mechanistic studies associated with the gain or loss of function in different genes	Limited availability; limited to a specific genetic alteration and small animals
	Pulmonary embolism (acute PH) or repeated embolism (chronic PH) via thrombus induction/microspheres	Rat, rabbit, sheep, pig	Simplicity, acute and chronic model	In the chronic model, mild hemodynamic severity without significant RV remodeling
	Acute occlusion of the pulmonary branch (surgery/balloon)	Rat, rabbit, sheep, dog, pig	Controlled afterload elevation	Does not reproduce human pathophysiology
	Pulmonary vein banding	Pig	Generates chronic postcapillary PH with arterial and venous and RV remodeling. Stable hemodynamic magnitude, useful for assessing therapies without their potential interference with the left ventricle	Need for surgery, anatomical variations in size and number of pulmonary veins; expensive. The absence of LV disease limits their translation (greater similarity to pulmonary vein or mitral stenosis)
Aortopulmonary shunt	Pig	Reproduces precapillary PH with vascular and biventricular remodeling. Stable hemodynamic magnitude; useful for treatment assessment	Complex surgery; high cost; absence of isolated right involvement (coexistence with volume overload and left remodeling)	
Pressure overload without PH	Stenosis (banding) of the PA	Mouse, rat, rabbit, sheep, dog, pig	Allows study of adaptive RV hypertrophy	Certain variability depending on the degree of the initial constriction triggered by the banding and the growth rhythm of the animal; need for surgery
<i>Volume overload</i>				
Right valve regurgitation (tricuspid or pulmonary)		Sheep, pig	Useful for pathophysiological study of isolated volume overload (acute and chronic); possibility of percutaneous procedures (less invasive)	Expensive; length of time to development of RV remodeling
Aortocaval shunt		Rat, mouse, dog, pig	Reproduces human pathophysiology (congenital heart diseases)	Need for surgery; mixed model (possible PH due to pulmonary overcirculation); long time to development of RV remodeling
<i>Cardiomyopathy</i>				
RV infarction (surgical ligation, occlusion, or coil implantation in the right coronary artery)		Rat, dog, pig	Reproduces the pathophysiology of a right coronary artery infarction in patients	Need for surgery or percutaneous procedure; high mortality (due to ventricular arrhythmias); variable infarct size (depending on coronary distribution) and concomitant left involvement
ARVC (transgenic models, mainly due to desmosomal mutations)		Rat, zebrafish	Useful for mechanistic studies associated with the gain or loss of function in different genes	Limited availability; limited to a specific genetic alteration and thus far focused on the mouse
Tachycardia-induced cardiomyopathy due to rapid atrial or ventricular pacing		Dog, pig	Relatively simple	May trigger biventricular dysfunction; few studies focused on the right ventricle; reversible upon pacing cessation

ARVC, arrhythmogenic right ventricular cardiomyopathy; LV, left ventricular; PA, pulmonary artery; PAH, pulmonary arterial hypertension; PH, pulmonary hypertension; PPAR $\gamma$ , peroxisome proliferator-activated receptor gamma; RV, right ventricular; TGF $\beta$ 1, transforming growth factor beta 1.

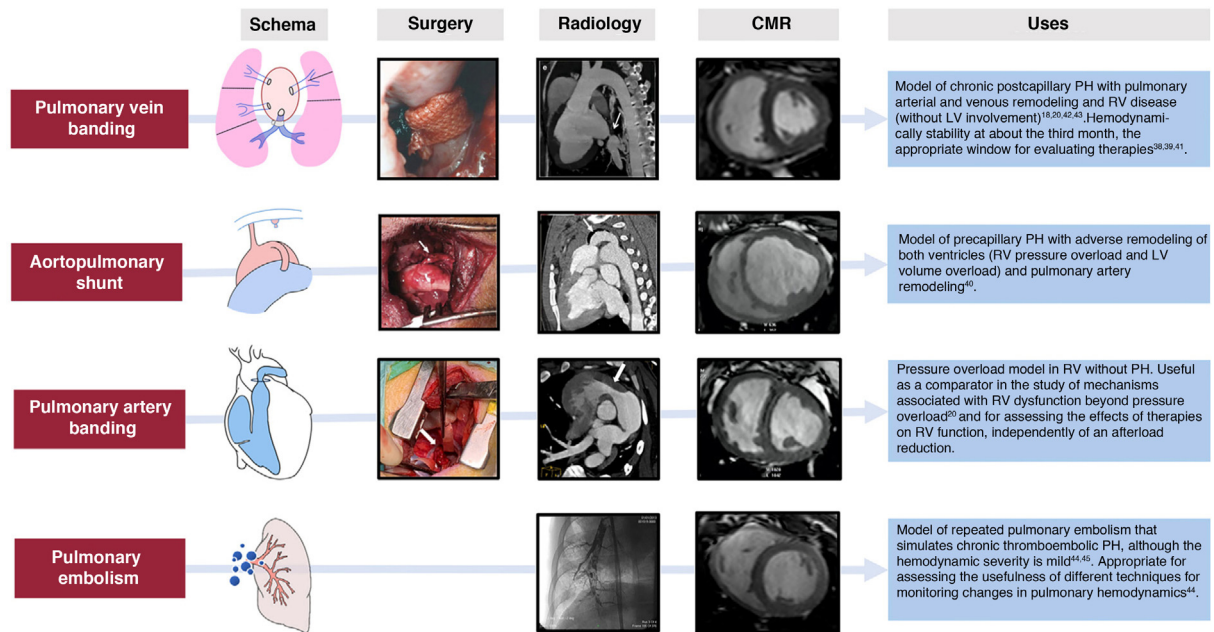


**Figure 4.** Porcine models of right ventricular pressure overload. CMR, cardiac magnetic resonance; LV, left ventricle; PH, pulmonary hypertension; RV, right ventricle.

## Multimodal imaging assessment

### Echocardiography

Echocardiography remains the most commonly used technique for the initial morphofunctional assessment of the right ventricle (figure 5). The dimensions to be measured are the basal, medial, and longitudinal diameters, the thickness of the free wall, the LV sphericity index, and the RV/LV basal diameter ratio. The probability of PH can be estimated using the peak tricuspid valve regurgitation velocity and the dimensions of the right atrium, right ventricle, PA, and inferior vena cava. The main parameters of RV function are described in table 4<sup>49–51</sup> with their normal values, advantages, and disadvantages. Tricuspid annular plane systolic excursion (TAPSE) and the peak systolic velocity of the lateral tricuspid annulus by tissue Doppler imaging ( $S'$ ) are easy to acquire and less dependent on the acoustic window. However, they have certain limitations when the RV contractility becomes preferentially circumferential, such as in PH<sup>52</sup> and after cardiac surgery.<sup>7</sup> The RV fractional area change shows a stronger correlation with RV ejection fraction (RVEF) on cardiac magnetic resonance (CMR) or computed tomography<sup>49,53</sup> but requires good delimitation of the endocardium. Analysis of longitudinal deformation (strain) using speckle tracking permits identification of subclinical dysfunction<sup>54</sup> and exhibits prognostic value in PH, tricuspid regurgitation, and HF.<sup>55</sup> The TAPSE/systolic pulmonary artery pressure ratio has been established as a noninvasive measure of RV-PA coupling<sup>56</sup> with prognostic value in HF and PH.<sup>3</sup> For the analysis of diastolic function, the  $E/A$  and  $Ee'$  indices from pulsed and tissue Doppler are used, as well as the peak strain rate in early diastole and RA strain.<sup>49</sup> Three-dimensional echocardiography is particularly useful in congenital heart diseases with single RV morphologies but its main limitation is its dependence on the acoustic window. Finally, stress echocardiography enables the evaluation of RV contractile reserve before surgery or a transcatheter valve intervention by analyzing changes in parameters such as TAPSE and  $S'$ .

### Cardiac magnetic resonance imaging

CMR is considered the gold standard for the noninvasive assessment of RV anatomy, function, and tissue characterization. Of the many parameters obtained (table 4),<sup>50,57</sup> the most frequently used in clinical practice is RVEF. An RVEF  $\leq 40\%$  in patients with acute myocardial infarction is a predictor of mortality, independently of age, infarct size, and LV ejection fraction.<sup>58</sup> A value  $< 45\%$  is associated with a higher incidence of cardiovascular events and shorter transplant-free survival in patients with dilated cardiomyopathy,<sup>5</sup> as well as higher hospitalization rates for HF and death after transcatheter tricuspid valve repair.<sup>59</sup> In addition, RVEF is a predictor of arrhythmic events and death in arrhythmogenic RV cardiomyopathy<sup>60</sup> and of major cardiovascular events in acute myocarditis.<sup>61</sup> RV global and segmental longitudinal strain can be evaluated using feature tracking (the most widely available modality), tagging, and fast strain-encoded CMR imaging (fast SENC).<sup>62</sup> In the difficult decision-making process regarding the optimal time to repair pulmonary regurgitation in corrected tetralogy of Fallot, an RV end-diastolic volume index of  $82 \text{ mL/m}^2$  indicates a high probability of reverse remodeling after intervention.<sup>27</sup> Other relevant cutoff points for clinical decision-making are included in table 2. Phase-contrast sequences permit accurate quantification of the ratio between pulmonary and systemic flow ( $Q_p/Q_s$ ) in patients with congenital shunts and the characterization of the PA flow and wall distensibility and could be used to estimate and monitor PVR.<sup>43,44</sup> The ratio of stroke volume to end-systolic volume is another noninvasive method for estimating RV-PA coupling.<sup>63</sup> Regarding tissue characterization, late gadolinium enhancement is frequently found at the RV insertion points and septum, correlating with hemodynamic severity in patients with PH, but it has no independent prognostic value.<sup>64</sup> In contrast, quantification of native  $T_1$  and the extracellular volume, which are surrogate parameters reflecting diffuse myocardial fibrosis, permit detection of early RV involvement<sup>18</sup> and has independent prognostic value.<sup>65</sup> New ultrafast sequences, such as Enhanced

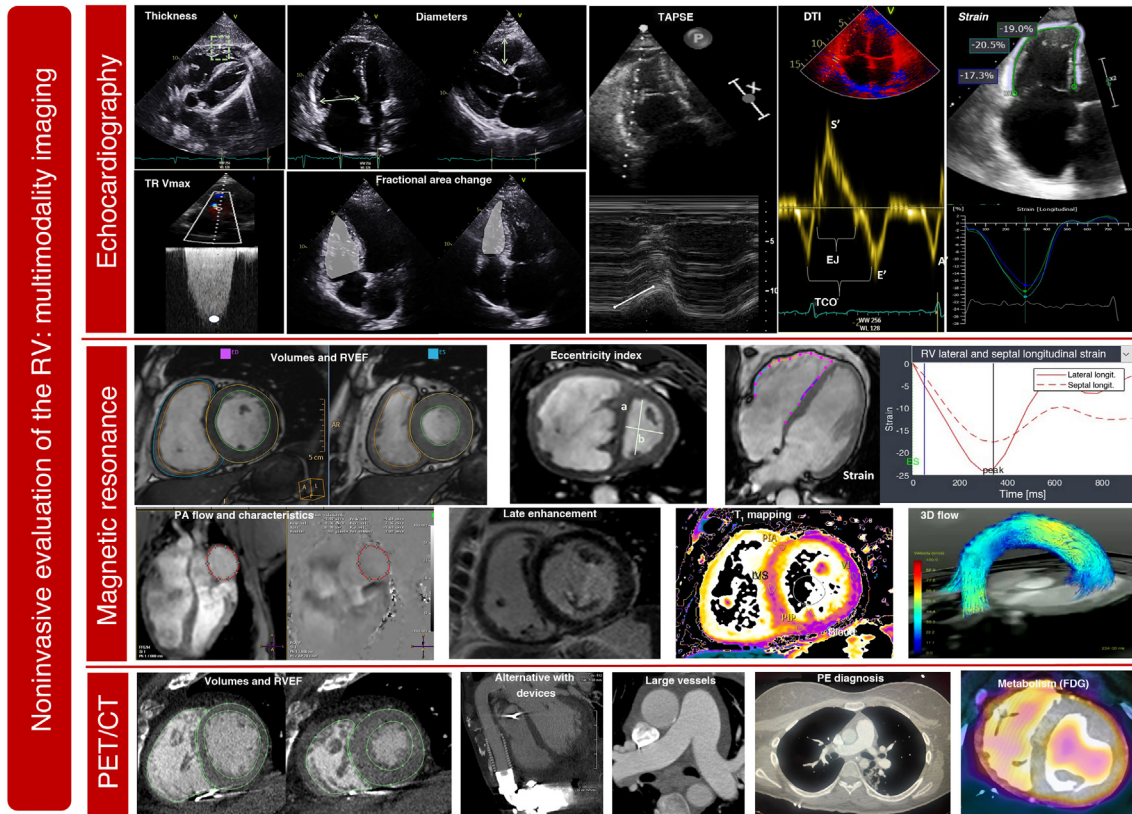
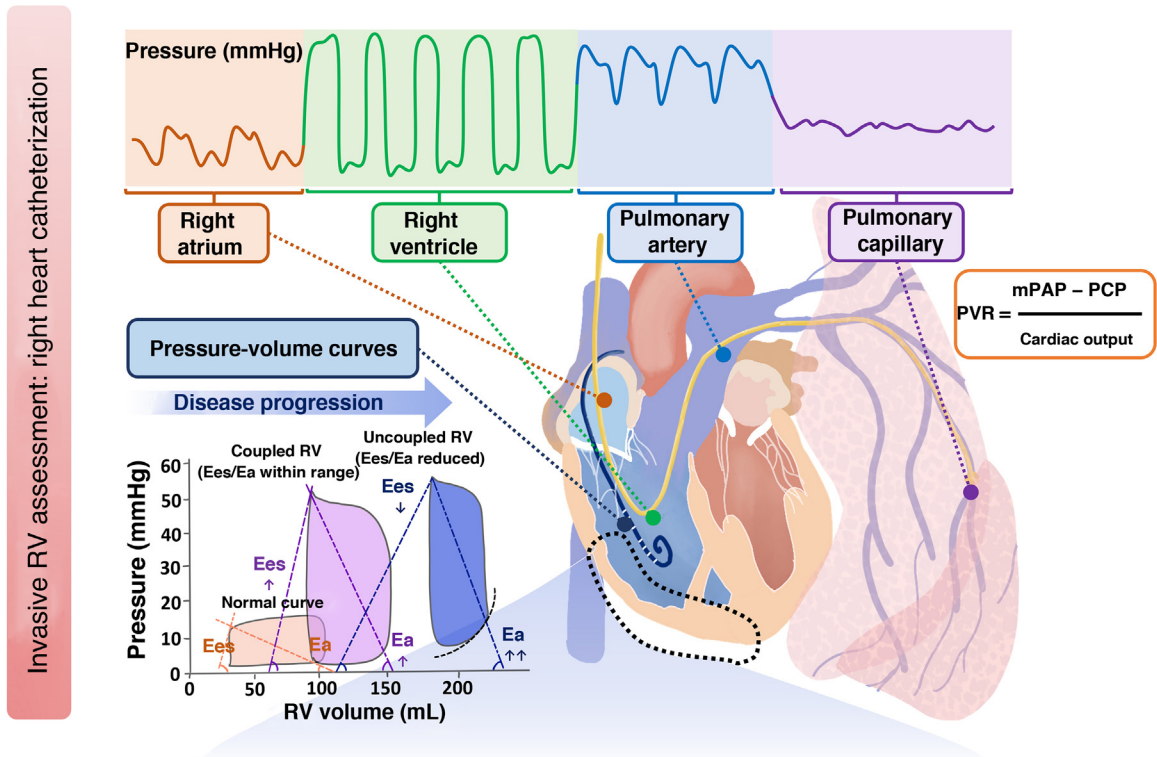


**Figure 5.** Main methods for assessing the right ventricle. A', late diastolic velocity of the mitral annulus; CT, computed tomography; E', early diastolic velocity of the mitral annulus; E<sub>a</sub>, effective arterial elastance; E<sub>es</sub>, end-systolic elastance; ED, end-diastole; ES, end-systole; ET, ejection time; FDG, fluorodeoxyglucose; IVS, interventricular septum; LV, left ventricle; mPAP, mean pulmonary arterial pressure; PA, pulmonary artery; PCP, pulmonary capillary pressure; PE, pulmonary embolism; PET, positron emission tomography; PIA, pulmonary inferior artery; PIP, posterior inferior papillary muscle; PVR, pulmonary vascular resistance; RVEF, right ventricular ejection fraction; RV, right ventricle; S', peak systolic velocity of the mitral annulus; TAPSE, tricuspid annular plane systolic excursion; TCO, tricuspid closure-opening time; TDI, tissue Doppler imaging; TR, tricuspid regurgitation; Vmax, maximal expiratory flow; WL, wall length; WW, wall-to-wall.

**Table 4**  
Most commonly used echocardiographic and cardiac magnetic resonance parameters for the functional evaluation of the right ventricle

	Reference values <sup>49</sup>	Uses and advantages	Limitations
<i>Echocardiography</i>			
TAPSE (M mode)	Normal: 24 ± 35 mm Abnormal: < 17 mm	- Assesses longitudinal contractility - Easy and quick; bedside test - Less dependent on the acoustic window - Prognostic value	- Does not consider radial function and ignores IVS and RVOT - Load-dependent - Not useful after surgery and heart transplant
TAPSE/sPAP	55-64 y: 0.89 ± 0.23 65-74 y: 0.84 ± 0.22 75-84 y: 0.77 ± 0.21 ≥ 85 y: 0.70 ± 0.22 (mm/mmHg)	- Noninvasively assesses RV/PA coupling - Prognostic value	- Not assessable in the absence of TR or if the TR is massive or torrential - Prognostic cutoff points depend on the clinical setting - Little evidence about normal values in healthy young individuals (< 55 y)
S' (tissue Doppler)	- Normal: 14.1 ± 2.3 cm/s - Abnormal: < 9.5 cm/s	- Assesses longitudinal contractility - Fast and reproducible - Prognostic value	- Similar limitations to TAPSE
Fractional area change	- Normal: 49% ± 7% - Abnormal: < 35%	- Assesses longitudinal and radial contractility - Good correlation with RVEF on CMR	- Requires good-quality images focused on the right ventricle and ignores RVOT - Load-dependent - Lower reproducibility
Myocardial performance index (tissue Doppler) (TCOT – ET)/ET	- Normal: 0.38 ± 0.08 - Abnormal: > 0.54	- Assesses RV systolic and diastolic function - Less dependent on the acoustic window; reproducible and fast	- Not reliable if the RA pressure is highly elevated
dP/dt	- Normal: ≤ 400 mmHg/s	- Easy and widely available	- Not applicable if TR is absent, massive, or torrential; load-dependent
RV free wall strain (by speckle tracking)	- Normal: –29% ± 4.5% - Abnormal: > –20%	- Assesses the longitudinal deformation of the free wall - Less dependent on load and acquisition angle conditions - Prognostic value	- Dependent on image quality and requires postprocessing - Does not include the RVOT - Manufacturer-dependent values (important for follow-up)
3D RVEF	- Normal: 58% ± 6.5% - Abnormal: < 45%	- Free of geometric assumptions - High correlation with CMR - Prognostic value	- Dependent on image quality and requires postprocessing - Less widely available and requires training
<i>CMR</i>			
RVEF	Men < 60 y: 64% ± 7%; LLN: < 50% Men ≥ 60 y: 69% ± 7%; LLN: < 55% Women < 60 y: 64% ± 6%; LLN: < 52% Women ≥ 60 y: 70% ± 6%; LLN: < 58%	- Free of geometric assumptions - Very useful for complex anatomies - Prognostic value	- Its conventional acquisition requires lengthy breath holds, limiting it to clinically stable patients - Less widely available and higher cost - Suboptimal acquisition in the presence of arrhythmias - Limited use in patients with incompatible devices, claustrophobia, chronic kidney disease, and gadolinium allergy - Requires training
<i>Right heart catheterization</i>			
Cardiac index	4.1 ± 1.3 L/min/m <sup>2</sup>	- Key parameter when considering the use of advanced mechanical support devices or transplant	- Measurement by thermodilution has limitations in the presence of significant TR or shunts - Fick's method requires physical assumptions that can lead to significant variability
Right atrial pressure	5.5 ± 2.0 mmHg	- Estimates RV preload - Provides data on patients' volume status and thus guides their management - A disproportionate elevation is a prognostic marker - V wave measurement: key for the planning of transcatheter tricuspid treatments	- Major variability based on patients' hemodynamic and volume status

**Table 4** (Continued)

Most commonly used echocardiographic and cardiac magnetic resonance parameters for the functional evaluation of the right ventricle

	Reference values <sup>49</sup>	Uses and advantages	Limitations
RAP/PCP	0.56 ± 0.07	- Measurement of the imbalance in the elevation of the RAP with respect to left chamber pressures, key for decision-making (transplantation and ventricular assistance) - A value > 0.64 is a risk factor for RV failure after ventricular assistance implantation	- Limited in patients with dysfunction of both ventricles because left and right filling pressures will both be elevated and the index may suggest normality
Pulmonary artery pulsatility index (PAPi) (sPAP – dPAP)/RAP	5.5 ± 4.4	- Validated in various studies in the context of advanced heart failure and as a predictor of RV failure after left ventricular assist device implantation as destination therapy - A value < 1.6 is a risk factor for RV failure after ventricular assist device implantation	- This parameter depends on pulmonary artery distensibility, RAP, and even stroke volume, hindering its comparison among individuals
RV stroke work index (RVSWI) (HF/HR) × (mPAP – RAP) × 0.00136	4–12 g/m/beat/m <sup>2</sup>	- A value < 4 is a risk factor for RV failure after ventricular assist device implantation	- This parameter depends on the preload and multiple parameters, which is why it exhibits greater variability and error

CMR, cardiac magnetic resonance; dPAP, diastolic pulmonary arterial pressure; ET, ejection time; HF, heart failure; HR, heart rate; IVS, interventricular septum; LLN, lower limit of normal; mPAP, mean pulmonary arterial pressure; PA, pulmonary artery; PAPi, pulmonary artery pulsatility index; PCP, pulmonary capillary pressure; RA, right atrial; RAP, right atrial pressure; RV, right ventricle; RVED, right ventricular ejection fraction; RVOT, right ventricular outflow tract; RVSWI, right ventricular stroke work index; sPAP, systolic pulmonary arterial pressure; TAPSE, tricuspid annular plane systolic excursion; TCO, tricuspid closure-opening time; TR, tricuspid regurgitation.

SENSE by Static Outer volume Subtraction (ESSOS), drastically reduce acquisition times without compromising quality,<sup>66</sup> permitting the more widespread use of CMR evaluation of the right ventricle.

#### Computed tomography

Clinically, computed tomography is most useful for diagnosing the causes of acute and chronic RV dysfunction, such as acute pulmonary embolism and chronic thromboembolic PH. However, in these cases, the study is typically not synchronized, limiting the data obtained on the right ventricle. In selected patients who are contraindicated for CMR and with insufficient information from echocardiography, as can occur in patients with ventricular assist devices,<sup>53</sup> synchronized retrospective computed tomography is a viable option because it enables the assessment of volumes, mass, and RVEF, with the downside of increased exposure to ionizing radiation.

#### Positron emission tomography

Although its use is still limited to research, this technique can be used to assess RV myocardial metabolism. In patients with PAH, more intense <sup>18</sup>F-fluorodeoxyglucose uptake has been associated with higher pressure overload, greater dysfunction, and a worse clinical course. PAH can be modified with vasodilator therapy.<sup>21</sup> Elevated septal uptake has also been found in patients with volume overload due to an atrial septal defect.<sup>23</sup>

#### Hemodynamic assessment of the right ventricle

Pressure-volume curves (figure 5) are the gold standard for evaluating RV function but have remained relegated to research due to their relative complexity (requiring a conductance catheter to be advanced to the right ventricle). Nonetheless, understanding their interpretation is valuable. Given that the X-axis indicates the volume and the Y-axis indicates the pressure, the width of the curve reflects the RV systolic volume while its area represents the stroke work. End-systolic elastance ( $E_{es}$ ) is the reference parameter

for assessing RV contractility, as it is independent of the pre- and afterload, and is obtained from the slope of the line connecting the end-systolic points of each curve. At the same time, effective arterial elastance ( $E_a$ ) is the most reliable parameter for RV afterload because it takes into account the resistive, pulsatile, and passive components of the right ventricle. This parameter is obtained as the slope of the line connecting the end-systolic and end-diastolic points of the curve. The  $E_{es}/E_a$  ratio represents RV-PA coupling. Its normal value is 1.  $E_{es}/E_a$  values less than 0.6 to 0.8 have been associated with poor outcomes in patients with pressure or volume overload.<sup>67,68</sup>

Right heart catheterization provides various RV functional parameters that are helpful for decision-making (table 2) and have prognostic value. The most important parameters are RA pressure, the ratio between RA pressure and pulmonary capillary pressure, the RV stroke work index ( $[(\text{cardiac index}/\text{heart rate}) \times (\text{mPAP} - \text{RA pressure}) \times 0.00136]$ ) and the PA pulsatility index (PAPi), which is calculated with the formula  $[(\text{systolic PAP} - \text{diastolic PAP})/\text{RA pressure}]$ . The normal values obtained from healthy individuals or the control groups of various studies are shown in table 4.<sup>51</sup> PAPi has acquired growing importance in recent years, largely in patients with cardiogenic shock or HF<sup>69</sup> and before implantation of an LV assist device.<sup>30</sup>

#### MANAGEMENT OF RIGHT VENTRICULAR DYSFUNCTION

The management of RV dysfunction is largely based on treating the underlying cause and optimizing preload, afterload, and contractility (figure 2).

#### Management of acute right ventricular dysfunction

The management of acute RV dysfunction must focus on hemodynamic support and controlling the cause. First, optimization of blood volume is key, given that excessive fluid administration can overdilate the right ventricle and increase its wall tension. This decreases contractility and worsens tricuspid regurgitation and ventricular interdependence, hindering LV filling

and thereby reducing cardiac output. Accordingly, although fluid administration may initially be necessary, volume status should be thoroughly and repeatedly assessed clinically or via measurement of central venous pressure.<sup>70</sup> In patients with signs of congestion or elevated central venous pressure, diuretic therapy must be started and then monitored and adjusted with the same caution.

Vasoconstrictor and inotropic therapy is indicated in patients with hemodynamic instability. Among vasoconstrictors, noradrenaline is preferred because it increases systemic blood pressure and coronary artery perfusion without affecting PVR. The most valuable inotropic agents are dobutamine, levosimendan, and milrinone. Levosimendan enhances ventriculoatrial coupling by increasing RV contractility and reducing afterload due to PA vasodilation.<sup>1</sup> In some cases, to reduce the afterload even further, selective pulmonary vasodilators can be used, such as nitric oxide and prostacyclins.<sup>1</sup> If the hemodynamic instability persists and is refractory to medical therapy, it is essential to consider the need for mechanical circulatory support at the optimal time. The choice of device depends on the estimated duration of support. Short-term devices include extracorporeal membrane oxygenation, the Impella RP (Abiomed, United States), and the PROTEK Duo (TandemLife, United States). If support is expected to exceed 10 to 15 days, surgically implanted devices, such as the Levitronix CentriMag (Abbott Medical, United States), should be chosen. In patients with an assisted RV who are not expected to recover, suitability for heart or heart-lung transplant must be assessed.<sup>1</sup>

In addition to these general measures, the underlying issue must be treated. Pulmonary embolism is one of the most frequent causes of acute RV dysfunction and, in high-risk patients—defined as those with hemodynamic instability caused by right HF—reperfusion therapy is indicated. This can be achieved through systemic or local transcatheter fibrinolysis, or percutaneous or surgical thrombectomy.<sup>24,71</sup> In RV infarction, the culprit artery must be revascularized as soon as possible; however, this approach may still be beneficial in the subacute phase given the more prolonged myocardial viability of the right ventricle.<sup>70</sup>

### Management of chronic right ventricular dysfunction

The management of chronic right HF requires a balanced diuretic approach that avoids congestion, and its renal and hepatic consequences while avoiding excessive fluid depletion that lowers cardiac output. In patients with diuretic resistance, sequential nephron blockade can be achieved by combining different classes of diuretics, such as loop diuretics, thiazides, mineralocorticoid receptor antagonists, acetazolamide, sodium-glucose cotransporter 2 inhibitors, and even vaptans; in patients with more advanced forms, hemodialysis or peritoneal dialysis should be considered.<sup>72</sup> In cardiohepatic syndrome, patients may exhibit a vasoplegic and hyperdynamic output phenotype, which is difficult to manage and has a poor prognosis.<sup>73</sup>

Currently, there is a lack of specific treatments for RV dysfunction. In chronic PH, the management of pressure overload depends on the etiological group.<sup>3</sup> In group 1 PH, specific pulmonary vasodilators are used that act on the endothelial 1, prostacyclin, and nitric oxide pathways. In contrast, in groups 2 and 3 PH, the priority is management of the underlying heart or lung disease. Finally, in group 4 patients, the anticoagulation and medical (riociguat), surgical, or percutaneous therapy depend on patient anatomy and characteristics.

In RV dysfunction due to volume overload, found in patients with tricuspid regurgitation, pulmonary regurgitation (frequent after tetralogy of Fallot repair), or intracardiac shunts, the indication for intervention and procedure (percutaneous or

surgical) should be individualized based on patient characteristics (eg, frailty), valve anatomy, and RV defect and function (table 2).

## CONCLUSIONS AND FUTURE DIRECTIONS

The right ventricle is unique in terms of its embryology, anatomy, and function. Although interest in this structure has grown exponentially in recent years, major challenges persist, such as how to better understand the mechanisms underlying the transition from adaptive remodeling to RV dysfunction, improving early diagnosis and treatment, and the identification of new therapeutic targets or procedures that improve prognosis. These challenges highlight the importance of translational research in the study of the right ventricle, opening the door to a burgeoning field of research posed to offer insights and solutions.

## FUNDING

This manuscript has been partially funded by the *Instituto de Salud Carlos III* with funding from the European Union via projects PI20/00742 and PI23/01341. The National Cardiovascular Research Center Carlos III receives funding from the *Instituto de Salud Carlos III*, the Spanish Ministry of Science and Innovation, and the *Fundación Pro CNIC* (AEI/10.13039/501100011033).

## STATEMENT ON THE USE OF ARTIFICIAL INTELLIGENCE

No artificial intelligence was used in the preparation of this manuscript.

## AUTHORS' CONTRIBUTIONS

All authors contributed to the design of the article and decisions about scientific content. C. Real and C.N. Pérez-García wrote the first draft of the manuscript; both authors contributed equally to this article. C. Galán-Arriola created the figures and contributed to the drafting and revision of the experimental animal model section. I. García-Lunar contributed to the drafting of the article and its revision, particularly the cardiac imaging section. A. García-Álvarez drafted the table of contents and performed a comprehensive review of the entire document.

## CONFLICTS OF INTEREST

None.

## REFERENCES

- Konstam MA, Kiernan MS, Bernstein D, et al. Evaluation and Management of Right-Sided Heart Failure: A Scientific Statement From the American Heart Association. *Circulation*. 2018;137:e578–e622.
- Obokata M, Reddy YNV, Melenovsky V, Pislaru S, Borlaug BA. Deterioration in right ventricular structure and function over time in patients with heart failure and preserved ejection fraction. *Eur Heart J*. 2019;40:689–697.
- McDonagh TA, Metra M, Adamo M, et al. 2022 ESC Guidelines for the diagnosis and treatment of acute and chronic heart failure. *Eur Heart J*. 2022;43:3618–3731.
- Wen S, Pislaru C, Ommen SR, Ackerman MJ, Pislaru SV, Geske JB. Right Ventricular Enlargement and Dysfunction Are Associated With Increased All-Cause Mortality in Hypertrophic Cardiomyopathy. *Mayo Clin Proc*. 2022;97:1123–1133.
- Gulati A, Ismail TF, Jabbour A, et al. The Prevalence and Prognostic Significance of Right Ventricular Systolic Dysfunction in Nonischemic Dilated Cardiomyopathy. *Circulation*. 2013;128:1623–1633.
- Manca P, Cannatà A, Nuzzi V, et al. Prevalence and Evolution of Right Ventricular Dysfunction Among Different Genetic Backgrounds in Dilated Cardiomyopathy. *Can J Cardiol*. 2021;37:1743–1750.

7. Moya Mur J-L, García Martín A, García Lledó A, et al. Geometrical and functional cardiac changes after cardiac surgery: a pathophysiological explanation based on speckle tracking. *Int J Cardiovasc Imaging*. 2018;34:1905-1915.
8. Haupt HM, Hutchins GM, Moore GW. Right ventricular infarction: role of the moderator band artery in determining infarct size. *Circulation*. 1983;67:1268-1272.
9. Waskova-Arnostova P, Elsnicova B, Kasparova D, et al. Right-To-Left Ventricular Differences in the Expression of Mitochondrial Hexokinase and Phosphorylation of Akt. *Cell Physiol Biochem*. 2013;31:66-79.
10. Wessels JN, van Wezenbeek J, de Rover J, et al. Right Atrial Adaptation to Precapillary Pulmonary Hypertension. *J Am Coll Cardiol*. 2023;82:704-717.
11. Yamaguchi S, Harasawa H, Li KS, Zhu D, Santamore WP. Comparative significance in systolic ventricular interaction. *Cardiovasc Res*. 1991;25:1714-1723.
12. Haddad F, Hunt SA, Rosenthal DN, Murphy DJ. Right Ventricular Function in Cardiovascular Disease. *Part I Circulation*. 2008;117:1436-1448.
13. Sadoshima J, Izumo S. The cellular and molecular response of cardiac myocytes to mechanical stress. *Annu Rev Physiol*. 1997;59:551-571.
14. Bogaard HJ, Abe K, Vonk Noordegraaf A, Voelkel NF. The Right Ventricle Under Pressure. *Chest*. 2009;135:794-804.
15. Stevens GR, García-Alvarez A, Sahni S, García MJ, Fuster V, Sanz J. RV Dysfunction In Pulmonary Hypertension Is Independently Related To Pulmonary Artery Stiffness. *JACC Cardiovasc Imaging*. 2012;5:378-387.
16. Grant B, Lieber B. Clinical significance of pulmonary arterial input impedance. *Eur Respir J*. 1996;9:2196-2199.
17. Andersen S, Nielsen-Kudsk JE, Vonk Noordegraaf A, de Man FS. Right Ventricular Fibrosis. *Circulation*. 2019;139:269-285.
18. García-Alvarez A, García-Lunar I, Pereda D, et al. Association of Myocardial T1-Mapping CMR With Hemodynamics and RV Performance in Pulmonary Hypertension. *JACC Cardiovasc Imaging*. 2015;8:76-82.
19. Kasimir M. Reverse cardiac remodelling in patients with primary pulmonary hypertension after isolated lung transplantation. *Eur J Cardio-Thoracic Surg*. 2004;26:776-781.
20. García-Lunar I, Jorge I, Sáiz J, et al. Metabolic changes contribute to maladaptive right ventricular hypertrophy in pulmonary hypertension beyond pressure overload: an integrative imaging and omics investigation. *Basic Res Cardiol*. 2024. <http://dx.doi.org/10.1007/s00395-024-01041-5>.
21. Oikawa M, Kagaya Y, Otani H, et al. Increased [18F]Fluorodeoxyglucose Accumulation in Right Ventricular Free Wall in Patients With Pulmonary Hypertension and the Effect of Epoprostenol. *J Am Coll Cardiol*. 2005;45:1849-1855.
22. Szabó G, Soós P, Bährle S, et al. Adaptation of the Right Ventricle to an Increased Afterload in the Chronically Volume Overloaded Heart. *Ann Thorac Surg*. 2006;82:989-995.
23. Otani H, Kagaya Y, Yamane Y, et al. Long-Term Right Ventricular Volume Overload Increases Myocardial Fluorodeoxyglucose Uptake in the Interventricular Septum in Patients With Atrial Septal Defect. *Circulation*. 2000;101:1686-1692.
24. Konstantinides SV, Meyer G, Becattini C, et al. 2019 ESC Guidelines for the diagnosis and management of acute pulmonary embolism developed in collaboration with the European Respiratory Society (ERS). *Eur Heart J*. 2020;41:543-603.
25. Vahanian A, Beyersdorf F, Praz F, et al. 2021 ESC/EACTS Guidelines for the management of valvular heart disease. *Eur Heart J*. 2022;43:561-632.
26. Baumgartner H, De Backer J, Babu-Narayan SV, et al. 2020 ESC Guidelines for the management of adult congenital heart disease. *Eur Heart J*. 2021;42:563-645.
27. Heng EL, Gatzoulis MA, Uebing A, et al. Immediate and Midterm Cardiac Remodeling After Surgical Pulmonary Valve Replacement in Adults With Repaired Tetralogy of Fallot. *Circulation*. 2017;136:1703-1713.
28. Soliman Oll, Akin S, Muslem R, et al. Derivation and Validation of a Novel Right-Sided Heart Failure Model After Implantation of Continuous Flow Left Ventricular Assist Devices: The EUROMACS (European Registry for Patients with Mechanical Circulatory Support) Right-Sided Heart Failure Risk Score. *Circulation*. 2018;137:891-906.
29. The Penn-Columbia Risk Score. University of Pennsylvania. Available at: <http://penncolumbiariskscore.weebly.com>. Accessed 20 May 2024.
30. Kang G, Ha R, Banerjee D. Pulmonary artery pulsatility index predicts right ventricular failure after left ventricular assist device implantation. *J Hear Lung Transplant*. 2016;35:67-73.
31. Babu-Narayan SV, Diller G-P, Gheta RR, et al. Clinical Outcomes of Surgical Pulmonary Valve Replacement After Repair of Tetralogy of Fallot and Potential Prognostic Value of Preoperative Cardiopulmonary Exercise Testing. *Circulation*. 2014;129:18-27.
32. Te Riele ASJM, James CA, Philips B, et al. Mutation-Positive Arrhythmogenic Right Ventricular Dysplasia/Cardiomyopathy: The Triangle of Dysplasia Displaced. *J Cardiovasc Electrophysiol*. 2013;24:1311-1320.
33. Austin KM, Trembley MA, Chandler SF, et al. Molecular mechanisms of arrhythmogenic cardiomyopathy. *Nat Rev Cardiol*. 2019;16:519-537.
34. Bodez D, Ternacle J, Guellich A, et al. Prognostic value of right ventricular systolic function in cardiac amyloidosis. *Amyloid*. 2016;23:158-167.
35. Keramida K, Lazaros G, Nihoyannopoulos P. Right ventricular involvement in hypertrophic cardiomyopathy: Patterns and implications. *Hell J Cardiol*. 2020;61:3-8.
36. Smedema J, van Geuns R, Ector J, Heidbuchel H, Ainslie G, Crijns HJGM. Right ventricular involvement and the extent of left ventricular enhancement with magnetic resonance predict adverse outcome in pulmonary sarcoidosis. *ESC Hear Fail*. 2018;5:157-171.
37. Andersen A, van der Feen DE, Andersen S, Schultz JG, Hansmann G, Bogaard HJ. Animal models of right heart failure. *Cardiovasc Diagn Ther*. 2020;10:1561-1579.
38. García-Álvarez A, Pereda D, García-Lunar I, et al. Beta-3 adrenergic agonists reduce pulmonary vascular resistance and improve right ventricular performance in a porcine model of chronic pulmonary hypertension. *Basic Res Cardiol*. 2016;111:49.
39. García-Lunar I, Pereda D, Santiago E, et al. Effect of pulmonary artery denervation in postcapillary pulmonary hypertension: results of a randomized controlled translational study. *Basic Res Cardiol*. 2019;114:5.
40. Pereda D, García-Lunar I, Sierra F, et al. Magnetic Resonance Characterization of Cardiac Adaptation and Myocardial Fibrosis in Pulmonary Hypertension Secondary to Systemic-To-Pulmonary Shunt. *Circ Cardiovasc Imaging*. 2016;9:e004566.
41. Santiago-Vacas E, García-Lunar I, Solanes N, et al. Effect of sildenafil on right ventricular performance in an experimental large-animal model of postcapillary pulmonary hypertension. *Transl Res*. 2021;228:64-75.
42. Pereda D, García-Alvarez A, Sánchez-Quintana D, et al. Swine Model of Chronic Postcapillary Pulmonary Hypertension with Right Ventricular Remodeling: Long-Term Characterization by Cardiac Catheterization Magnetic Resonance, and Pathology. *J Cardiovasc Transl Res*. 2014;7:494-506.
43. García-Álvarez A, Fernández-Friera L, García-Ruiz JM, et al. Noninvasive Monitoring of Serial Changes in Pulmonary Vascular Resistance and Acute Vasodilator Testing Using Cardiac Magnetic Resonance. *J Am Coll Cardiol*. 2013;62:1621-1631.
44. García-Alvarez A, Fernández-Friera L, Mirelis JG, et al. Non-invasive estimation of pulmonary vascular resistance with cardiac magnetic resonance. *Eur Heart J*. 2011;32:2438-2445.
45. Agüero J, Ishikawa K, Fish KM, et al. Combination Proximal Pulmonary Artery Coiling and Distal Embolization Induces Chronic Elevations in Pulmonary Artery Pressure in Swine. *PLoS One*. 2015;10:e0124526.
46. Borgdorff MAJ, Dickinson MG, Berger RMF, Bartelds B. Right ventricular failure due to chronic pressure load: What have we learned in animal models since the NIH working group statement?. *Heart Fail Rev*. 2015;20:475-491.
47. Troughton RW, Prior DL, Pereira JJ, et al. Plasma B-type natriuretic peptide levels in systolic heart failure. *J Am Coll Cardiol*. 2004;43:416-422.
48. Scheel PJ, Florido R, Hsu S, et al. Safety and Utility of Cardiopulmonary Exercise Testing in Arrhythmogenic Right Ventricular Cardiomyopathy/Dysplasia. *J Am Heart Assoc*. 2020;9:e013695.
49. Hahn RT, Lerakis S, Delgado V, et al. Multimodality Imaging of Right Heart Function. *J Am Coll Cardiol*. 2023;81:1954-1973.
50. Kawel-Boehm N, Maceira A, Valsangiacomo-Buechel ER, et al. Normal values for cardiovascular magnetic resonance in adults and children. *J Cardiovasc Magn Reson*. 2015;17:29.
51. Wolsk E, Bakkestøm R, Thomsen JH, et al. The Influence of Age on Hemodynamic Parameters During Rest and Exercise in Healthy Individuals. *JACC Hear Fail*. 2017;5:337-346.
52. Kind T, Mauritz G-J, Marcus JT, van de Veerdonk M, Westerhof N, Vonk-Noordegraaf A. Right ventricular ejection fraction is better reflected by transverse rather than longitudinal wall motion in pulmonary hypertension. *J Cardiovasc Magn Reson*. 2010;12:35.
53. García-Alvarez A, Fernández-Friera L, Lau JF, et al. Evaluation of right ventricular function and post-operative findings using cardiac computed tomography in patients with left ventricular assist devices. *J Hear Lung Transplant*. 2011;30:896-903.
54. Mingo-Santos S, Moñivas-Palmero V, García-Lunar I, et al. Usefulness of Two-Dimensional Strain Parameters to Diagnose Acute Rejection after Heart Transplantation. *J Am Soc Echocardiogr*. 2015;28:1149-1156.
55. Houard L, Benaets M-B, de Meester de Ravenstein C, et al. Additional Prognostic Value of 2 D Right Ventricular Speckle-Tracking Strain for Prediction of Survival in Heart Failure and Reduced Ejection Fraction. *JACC Cardiovasc Imaging*. 2019;12:2373-2385.
56. Tello K, Wan J, Dalmer A, et al. Validation of the Tricuspid Annular Plane Systolic Excursion/Systolic Pulmonary Artery Pressure Ratio for the Assessment of Right Ventricular-Arterial Coupling in Severe Pulmonary Hypertension. *Circ Cardiovasc Imaging*. 2019;12:e009047.
57. Real C, Párraga R, Pizarro G, et al. Magnetic resonance imaging reference values for cardiac morphology, function and tissue composition in adolescents. *eClinicalMedicine*. 2023;57:101885.
58. Larose E, Ganz P, Reynolds HG, et al. Right Ventricular Dysfunction Assessed by Cardiovascular Magnetic Resonance Imaging Predicts Poor Prognosis Late After Myocardial Infarction. *J Am Coll Cardiol*. 2007;49:855-862.
59. Kresoja K-P, Rommel K-P, Lücke C, et al. Right Ventricular Contraction Patterns in Patients Undergoing Transcatheter Tricuspid Valve Repair for Severe Tricuspid Regurgitation. *JACC Cardiovasc Interv*. 2021;14:1551-1561.
60. te Riele ASJM, Bhonsale A, James CA, et al. Incremental Value of Cardiac Magnetic Resonance Imaging in Arrhythmic Risk Stratification of Arrhythmogenic Right Ventricular Dysplasia/Cardiomyopathy-Associated Desmosomal Mutation Carriers. *J Am Coll Cardiol*. 2013;62:1761-1769.
61. Bernhard B, Schnyder A, Garachemani D, et al. Prognostic Value of Right Ventricular Function in Patients With Suspected Myocarditis Undergoing Cardiac Magnetic Resonance. *JACC Cardiovasc Imaging*. 2023;16:28-41.
62. Real C, Párraga R, González-Calvo E, et al. Adolescent Reference Values for MR-Derived Biventricular Strain Obtained Using Feature-Tracking and Myocardial Tagging. *J Magn Reson Imaging*. 2024. <http://dx.doi.org/10.1002/jmri.29334>.
63. Sanz J, García-Alvarez A, Fernández-Friera L, et al. Right ventriculo-arterial coupling in pulmonary hypertension: a magnetic resonance study. *Heart*. 2012;98:238-243.
64. Swift AJ, Rajaram S, Capener D, et al. LGE Patterns in Pulmonary Hypertension Do Not Impact Overall Mortality. *JACC Cardiovasc Imaging*. 2014;7:1209-1217.
65. Nitsche C, Kammerlander AA, Binder C, et al. Native T1 time of right ventricular insertion points by cardiac magnetic resonance: relation with invasive haemody-

- namics and outcome in heart failure with preserved ejection fraction. *Eur Hear J - Cardiovasc Imaging*. 2020;21:683–691.
66. Gómez-Talavera S, Fernández-Jiménez R, Fuster V, et al. Clinical Validation of a 3-Dimensional Ultrafast Cardiac Magnetic Resonance Protocol Including Single Breath-Hold 3-Dimensional Sequences. *JACC Cardiovasc Imaging*. 2021;14:1742–1754.
  67. Richter MJ, Peters D, Ghofrani HA, et al. Evaluation and Prognostic Relevance of Right Ventricular–Arterial Coupling in Pulmonary Hypertension. *Am J Respir Crit Care Med*. 2020;201:116–119.
  68. Tello K, Dalmer A, Axmann J, et al. Reserve of Right Ventricular–Arterial Coupling in the Setting of Chronic Overload. *Circ Heart Fail*. 2019;12:e005512.
  69. Kochav SM, Flores RJ, Truby LK, Topkara VK. Prognostic Impact of Pulmonary Artery Pulsatility Index (PAPi) in Patients With Advanced Heart Failure: Insights From the ESCAPE Trial. *J Card Fail*. 2018;24:453–459.
  70. Harjola V, Mebazaa A, Čelutkienė J, et al. Contemporary management of acute right ventricular failure: a statement from the Heart Failure Association and the Working Group on Pulmonary Circulation and Right Ventricular Function of the European Society of Cardiology. *Eur J Heart Fail*. 2016;18:226–241.
  71. Real C, Ferrera C, Vázquez-Álvarez ME, et al. Reperfusion therapies in patients with intermediate and high-risk pulmonary embolism: insights from a multicenter registry. *REC Interv Cardiol*. 2024. <http://dx.doi.org/10.24875/RECI-CE.M24000452>.
  72. Testani JM, Khera AV, St. John Sutton MG, et al. Effect of Right Ventricular Function and Venous Congestion on Cardiorenal Interactions During the Treatment of Decompensated Heart Failure. *Am J Cardiol*. 2010;105:511–516.
  73. Xanthopoulos A, Starling RC, Kitai T, Triposkiadis F. Heart Failure and Liver Disease. *JACC Hear Fail*. 2019;7:87–97.